AIMS Mathematics, 10(8): 17657–17671.
DOI: 10.3934/math.2025789
Received: 06 March 2025
Revised: 20 July 2025
Accepted: 28 July 2025
Published: 05 August 2025

https://www.aimspress.com/journal/Math

Research article

The numerical solution of the Dirichlet generalized and classical harmonic problems for irregular n-sided pyramidal domains by the method of probabilistic solutions

Mamuli Zakradze[1], Zaza Tabagari[1], Nana Koblishvili[1], Tinatin Davitashvili[2], José-María Sánchez-Sáez[3] and Francisco Criado-Aldeanueva[4,*]

[1] Department of Computational Methods, N. Muskhelishvili Institute of Computational Mathematics of the Georgian Technical University, Tbilisi, Georgia

[2] Faculty of Exact and Natural Sciences, I. Javakhishvili Tbilisi State University, Tbilisi, Georgia

[3] Department of Didactics of Mathematics, Faculty of Education, University of Malaga, 29071 Malaga, Spain

[4] Department of Applied Physics II, Polytechnic School, University of Malaga, 29071 Malaga, Spain

* **Correspondence:** Email: fcriado@uma.es.

Abstract: This paper describes the application of the method of probabilistic solutions (MPS) to numerically solve the Dirichlet generalized and classical harmonic problems for irregular n-sided pyramidal domains. Here, "generalized" means that the boundary function has a finite number of first-kind discontinuity curves, with the pyramid edges acting as these curves. The pyramid's base is a convex polygon, and its vertex projection lies within the base. The proposed algorithm for solving boundary problems numerically includes the following steps: a) applying MPS, which relies on computer modeling of the Wiener process; b) determining the intersection point between the simulated Wiener process path and the pyramid surface; c) developing a code for numerical implementation and verifying the accuracy of the results; d) calculating the desired function's value at any chosen point. Two examples are provided for illustration, and the results of the numerical experiments are presented and discussed.

Keywords: Dirichlet generalized and classical harmonic problems; method of probabilistic solution; Wiener process; pyramidal domain
Mathematics Subject Classification: 35J05, 35J25, 65C30, 65N75

1. Introduction

In practical stationary problems, such as determining the temperature of a thermal field or the potential of an electric field, it is sometimes necessary to consider the Dirichlet generalized harmonic problem (see e.g., [1, 2, 11]).

Typically the methods (see e.g., [6,7]) used for obtaining numerical solutions to classical boundary-value problems are: a) less suitable or b) ineffective and sometimes useless for solving generalized boundary problems. The approximate solution of the generalized problem has low accuracy in the first case due to very slow convergence of the approximation process near discontinuity curves (see e.g., [1, 2, 11]). The similar issue occurs in the second case when solving the three-dimensional Dirichlet generalized harmonic problem using the MFS.

Researchers have attempted preliminary "improvements" to address the boundary value problem at hand. For Dirichlet plane generalized harmonic problems, the following methods have been developed: I) The method to reduce the Dirichlet generalized harmonic problem to a classical problem (see e.g., [8, 12]); II) The method of conformal mapping (see e.g., [10]); and III) The method of probabilistic solution (see e.g., [3, 5]). For three-dimensional Dirichlet generalized harmonic problems, only the third method is applicable.

Researchers encounter more significant challenges with three-dimensional Dirichlet generalized harmonic problems. Specifically, there is no universal approach that can be applicable to a broad class of spatial domains.

The aforementioned references [1, 2, 11] address relatively simple problems. Primarily, heuristic methods, the method of separation of variables, and particular solutions are used for their solution, resulting in low accuracy. Heuristic methods can sometimes provide incorrect solutions, requiring verification to ensure all problem conditions are met (see e.g., [6]). Consequently, the development of effective computational schemes with high accuracy for the numerical solution of three-dimensional Dirichlet generalized harmonic problems –that can be applied to a wide range of spatial domains– holds both theoretical and practical significance.

It is important to note that in [9], the discontinuity curves are disregarded while solving Dirichlet generalized harmonic problems for a sphere. This oversight, along with the use of classical methods, is the primary reason for the low accuracy. Thus, for the approximate solution of three-dimensional Dirichlet generalized harmonic problems, one should use methods that do not require approximating the boundary function and are applicable when discontinuity curves exist. One such methods is the method of probabilistic solutions (MPS).

Note that our interest in the numerical solution of both generalized and classical harmonic Dirichlet problems for pyramidal regions using the MPS method stems from the following observation: the existing literature [1, 2, 11] does not address either the generalized or classical problems for pyramidal domains. We believe this omission is likely due to the geometric complexity of the pyramid.

This observation sparked greater interest in the topic. We began by developing an appropriate approach for the approximate solution of the aforementioned problems for a regular n-sided pyramid using the MPS method. Then, we successfully developed the algorithm, which was applied to solve problems for both a complete pyramid in the case of $n = 4, 6$, and a regular truncated pyramid in the case of $n = 5$ (see [15]).

We continued our research in the case of irregular n-sided pyramids to solve the same problems

using the MPS method. Specifically, we examined two cases:

(1) An irregular 3-sided pyramid, where the height coincides with a lateral edge, lying along the Ox_3 axis, with the base on Ox_1x_2 plane, and the angle between side faces containing the height is $\pi/2$ (in all cases considered, the pyramid's edges are supposed to be the lines of discontinuity);
(2) An irregular 4-sided pyramid with a rectangular base located in the first quadrant of the Ox_1x_2 plane, where the vertex projection lies at the center of the base.

Numerical solutions of these examples using MPS revealed that, unlike regular pyramids (see [15]), solving generalized and classical Dirichlet harmonic problems for irregular pyramids requires an individual approach (see [19]).

In [20], the problem of finding the numerical solution for both generalized and classical harmonic Dirichlet problems in a spatially finite region using the MPS method, particularly at points near the boundary, and the impact of quantization number nq on solution accuracy, is studied. The research focused on a specific type of irregular 3-sided pyramidal region, where all edges are first-order discontinuity lines (as in the previously discussed examples), and the height coincides with a lateral edge. Additionally, the angle between faces containing the height is $\pi/4$. Numerical experiments demonstrated that achieving an accurate numerical solution near the boundary requires an optimal selection of the quantization number nq for each point, balancing both solution accuracy and computational efficiency.

Finally, we developed an appropriate algorithm for solving the numerical problems using the MPS method, followed by conducting numerical experiments. The results of this work are presented in this paper.

The present paper is structured as follows: Section 2 presents the formulation of the three-dimensional Dirichlet generalized harmonic problem. Section 3 briefly describes the MPS and Wiener process simulation. In Section 4 the algorithm for finding the intersection point between the simulated Wiener process trajectory and the surface of the pyramid is detailed. An auxiliary classical problem is examined in Section 5. Section 6 presents the results of numerical examples. Finally, Section 7 offers conclusions and suggestions for future research.

2. Formulation of the generalized problem

Let D be the interior of an irregular n-sided pyramid $P_n(h) \equiv P_n$ in R^3 space. By h is denoted its height, passing through the base of P_n. Without loss of generality we assume that h is aligned with Ox_3 in the right-handed Cartesian coordinate system $Ox_1x_2x_3$ and P_n's base lies in the plane Ox_1x_2.

Additionally, suppose the vertices of the base $A_1, A_2, \ldots, A_n$ of $P_n = MA_1A_2...A_n$ are arranged in a counter-clockwise direction, with the axis Ox_1 passing through vertex A_1. We will now formulate the following problem for the pyramid $P_n \equiv \overline{D}$. Similar to [15], we now state the following problem for the irregular pyramid P_n.

Problem 1. *Suppose the function $g(y)$, defined on the boundary S of the pyramid P_n, is continuous everywhere except along the edges $l_1, l_2, \ldots, l_{2n}$, of P_n, which represent first-kind discontinuity curves for $g(y)$. The goal is to find a function $u(x) \equiv u(x_1, x_2, x_3) \in C^2(D) \cap C(\overline{D} \setminus \cup_{k=1}^{2n} l_k)$ that satisfies the following conditions:*

$$\Delta u(x) = 0, \quad x \in D, \tag{2.1}$$

$$u(y) = g(y), \quad y \in S, \quad y\overline{\in} l_k \subset S \quad (k = 1, \ldots, 2n), \tag{2.2}$$

$$|u(x)| < c, \quad x \in \overline{D}, \tag{2.3}$$

where $\Delta = \sum_{i=1}^{3} \partial^2/\partial x_i^2$ *is the Laplace operator,* l_k $(k = 1, \ldots, 2n)$ *represents the edges of* P_n*, and* c *is a real constant.*

It has been demonstrated (see [4, 14]) that the problem (2.1)–(2.3) has a solution, which is unique and continuously depends on the given data. Moreover, there holds the generalized extremum principle for the generalized solution $u(x)$:

$$\min_{x\in S} u(x) < \underset{x\in D}{u(x)} < \max_{x\in S} u(x), \tag{2.4}$$

where it is assumed that $x\overline{\in} l_k (k = 1, \ldots, 2n)$, for $x \in S$.

Observe (refer to [14]) that the added (2.3) condition of boundedness applies specifically to the neighborhoods surrounding discontinuity curves of the function $g(y)$ and is crucial for the extremum principle (2.4).

According to (2.3), $u(y)$ values are typically undefined along the l_k curves. For example, if Problem 1 is concerned with determining the thermal or electric field, then we must take $u(y) = 0$ for $y \in l_k$. In this context, the l_k curves physically represent non-conductors (or dielectrics). Otherwise, they would not be considered as discontinuity curves.

It is evident that, in this approach, the boundary function $g(y)$ has the following form.

$$g(y) = \begin{cases} g_1(y), & y \in S_1 \\ g_2(y), & y \in S_2 \\ \vdots & \vdots \\ g_n(y), & y \in S_n \\ g_{n+1}(y), & y \in S_{n+1} \\ 0, & y \in l_k \ (k = 1, \ldots, 2n) \end{cases} \tag{2.5}$$

where: S_i $(i = 1, \ldots, n)$ are the lateral faces and S_{n+1} is the base of P_n, respectively, excluding the boundaries. The functions $g_i(y)$, $y \in S_i$ $(i = 1, \ldots, n + 1)$ are continuous on their respective S_i of S. Clearly, $S = (\cup_{i=1}^{n+1} S_i) \cup (\cup_{k=1}^{2n} l_k)$.

Remark 1.

a) The case of vacuum within the surface S corresponds to the generalized problem with respect to closed shells.
b) Not all edges of the pyramid must be dielectric in Problem 1. Furthermore, scenarios can be considered where faces, apothems, base diagonals, and other elements function as dielectrics.

3. Simulation of the Wiener process and the method of probabilistic solution

This section provides a brief overview of the algorithm for numerically solving problems of type 1, with a detailed description available in [16]. The key theorem that enables the application of the MPS is as follows (see e.g., [4]).

Theorem 1. *Suppose $g(y)$ is a continuous (or discontinuous) bounded function on S and the finite domain $D \subset \mathbb{R}^3$ is bounded by a piecewise smooth surface S; then the solution of the Dirichlet classical (or generalized) boundary value problem for the Laplace equation at the fixed point $x \in D$ is given by the following form.*

$$u(x) = E_x g(x(\tau)). \tag{3.1}$$

In Eq (3.1), it is assumed that the Wiener process starts at the point $x(t_0) = (x_1(t_0), x_2(t_0), x_3(t_0)) \in D$, where the value of the desired function is to be determined. $E_x g(x(\tau))$ represents the mathematical expectation of values of the boundary function $g(y)$ at the random intersection points between the Wiener process trajectory and the boundary S, and τ denotes the random moment at which the Wiener process $x(t) = (x_1(t), x_2(t), x_3(t))$ first exits the domain D. If N, the number of the random intersection points $y^i = (y_1^i, y_2^i, y_3^i) \in S \quad (i = 1, 2, \ldots, N)$ is sufficiently large, then by the law of large numbers, Eq (3.1) becomes:

$$u(x) \approx u_N(x) = \frac{1}{N} \sum_{i=1}^{N} g(y^i) \tag{3.2}$$

or $u(x) = \lim u_N(x)$ for $N \to \infty$, in a probability sense.

Therefore, in the case of the Wiener process, the approximate value of the probabilistic solution to Problem 1 at a point $x \in D$ is computed according to the formula (3.2).

To simulate the Wiener process, we employ the following recursion relations (see e.g., [16]):

$$\begin{gathered} x(t_0) = x, \\ \left.\begin{aligned} x_1(t_k) &= x_1(t_{k-1}) + \gamma_1(t_k)/nq, \\ x_2(t_k) &= x_2(t_{k-1}) + \gamma_2(t_k)/nq, \\ x_3(t_k) &= x_3(t_{k-1}) + \gamma_3(t_k)/nq, \end{aligned}\right\} k = 1, 2, \ldots. \end{gathered} \tag{3.3}$$

Following these relations, the coordinates of the point $x(t_k) = (x_1(t_k), x_2(t_k), x_3(t_k))$ are determined. In Eq (3.3), $\gamma_1(t_k), \gamma_2(t_k)$ and $\gamma_3(t_k)$ are three independent random numbers with a normal distribution for the k-th step, each with a mean of zero and a variance of one, and nq represents the number of quantification where $1/nq = \sqrt{t_k - t_{k-1}}$. As nq approaches infinity, the discrete process approximates the continuous Wiener process. In practice, the random process is simulated at each step of the walk and continues until it crosses the boundary.

In this paper, we use pseudo-random numbers generated in the MATLAB environment to solve Dirichlet boundary value problems for Laplace's equation.

4. Finding the intersection point of the trajectory of the simulated Wiener process and the surface S of the pyramid P_n

To determine the intersection points $y^j = (y_1^j, y_2^j, y_3^j)$ $(j = 1, \ldots, N)$ between the Wiener process trajectory and the surface S (see Section 3), we proceed as follows: First, during the implementation of the Wiener process, we need to check whether each current point $x(t_k)$ defined by Eq (3.3) is inside $\overline{P_n}$ ($\overline{P_n} = P_n \bigcup S$) or not.

To address this, we have two parameters, n and h, as well as the coordinates of vertices: $M = (0, 0, h)$, $A_1 = (a_1, b_1)$, $A_2 = (a_2, b_2)$,..., $A_n = (a_n, b_n)$ of P_n. Using these parameters, we need to find

(1) equations of lines passing through the neighboring vertices of the base, (2) the equations of lateral faces, and (3) the inclination angles α_m, $(m = 1, \ldots, n)$ of the lateral faces relative to the base plane of P_n.

We will derive the equations of lines that pass through the points A_m and A_{m+1} $(m = 1, \ldots, n$, $A_{n+1} \equiv A_1)$ in the following form.

$$x_2 = k_m x_1 + c_m. \tag{4.1}$$

Taking into account that $A_m = (a_m, b_m)$, $A_{m+1} = (a_{m+1}, b_{m+1})$, then for the definition of constants k_m and c_m in (4.1), we obtain the following algebraic system:

$$\begin{aligned} b_m &= k_m a_m + c_m, \\ b_{m+1} &= k_m a_{m+1} + c_m. \end{aligned} \tag{4.2}$$

It is easy to see that from (4.2)

$$k_m = \frac{b_m - b_{m+1}}{(a_m - a_{m+1})}, \qquad c_m = \frac{a_m b_{m+1} - b_m a_{m+1}}{a_m - a_{m+1}}, \tag{4.3}$$

where if $m = n$, then $a_{n+1} = a_1, b_{n+1} = b_1$.

Without loss of generality, we assume that in (4.3), $a_m - a_{m+1} \neq 0$. Indeed, if $a_m - a_{m+1} = 0$, then the line $A_m A_{m+1}$ is perpendicular to Ox_1. In order to avoid this circumstance, it is enough to take such a vertex in the role of A_1 for which $a_m - a_{m+1} \neq 0$.

Now we find the equations of the planes passing through the points: $M(0, 0, h)$, A_m and A_{m+1}, $m = 1, \ldots, n$ (or the equations of the lateral faces of P_n).

It is well known that the equation of the plane passing through three points $P_1(x_1, y_1, z_1)$, $P_2(x_2, y_2, z_2)$, $P_3(x_3, y_3, z_3)$ has the following form:

$$\begin{vmatrix} x - x_1 & y - y_1 & z - z_1 \\ x_2 - x_1 & y_2 - y_1 & z_2 - z_1 \\ x_3 - x_1 & y_3 - y_1 & z_3 - z_1 \end{vmatrix} = 0. \tag{4.4}$$

In our case, in the role of the points: P_1, P_2 and P_3 we have $M(0, 0, h)$, $A_m(a_m, b_m, 0)$, and $A_{m+1}(a_{m+1}, b_{m+1}, 0)$, respectively. On the basis of (4.4), the equation of the plane passing through M, A_m, A_{m+1} has the following form:

$$\begin{vmatrix} x & y & z - h \\ a_m & b_m & -h \\ a_{m+1} & b_{m+1} & -h \end{vmatrix} = 0. \tag{4.5}$$

If we write (4.5) in system $Ox_1x_2x_3$ and carry out proper calculations, we will see that the equation has the following form:

$$h(b_{m+1} - b_m)x_1 - h(a_{m+1} - a_m)x_2 + (a_m b_{m+1} - a_{m+1} b_m)x_3 - (a_m b_{m+1} - a_{m+1} b_m)h = 0. \tag{4.6}$$

In particular, this refers to the equation of the m-th lateral face of P_n when $(x_1, x_2, x_3) \in \overline{S}_m$.

For the inclination angles α_m $(m = 1, \ldots, n)$ of the lateral faces relative to the base plane of P_n, we have $\alpha_m = \arctan(h/d_m)$, where d_m is the distance from the point O to the m-th side of the base of P_n and is given by the formula: $d_m = \text{abs}(c_m/\sqrt{1 + k_m^2}$, $(m = 1, \ldots, n)$.

With this information about the pyramid P_n, one can determine whether each current point $x(t_k)$, defined by Eq (3.3), is inside $\overline{P_n}$ or not. To do this, at each step of the simulated Wiener process, the angles β_m $(m = 1, \ldots, n)$ are calculated, which represent the angles of inclination of the planes that pass through the points $x(t_k)$, A_m, A_{m+1} relative to the base plane of P_n. It is evident that

$$\beta_m = \arctan(x_3(t_k)/\Delta_m),$$

where Δ_m represents a distance between the point $(x_1(t_k), x_2(t_k))$ and the line A_mA_{m+1}. It is known that

$$\Delta_m = \frac{|k_m x_1(t_k) - x_2(t_k) + c_m|}{\sqrt{k_m^2 + 1}}, \qquad m = 1, \ldots, n, \quad k = 1, 2, \ldots,$$

where k_m and c_m are defined by (4.3).

After calculating the angles β_m, they are compared with the angle α_m, $(m = 1, \ldots, n)$. Specifically:

1) If $\beta_m < \alpha_m$ and $0 < x_3(t_k) < h$ for $m = 1, \ldots, n$, then the process continues until it intersects the boundary S.
2) If for $m = p, \beta_p = \alpha_p$ and $0 < x_3(t_k) < h$ then $x(t_k) \in \overline{S_p}$ or $y^j = (y_1^j, y_2^j, y_3^j) = x(t_k)$.
3) If $\beta_p > \alpha_p$ and $0 < x_3(t_k) < h$, it indicates that the trajectory of the modulated Wiener process at the moment $t = t_{k-1}$ has intersected the p-th lateral face of P_n or that $x(t_{k-1}) \in P_n$ while for the moment $t = t_k$, $x(t_k) \overline{\in} \overline{P_n}$. In this case, to approximate the intersection point y^j, we first determine the parametric equation of the line L passing through $x(t_{k-1})$ and $x(t_k)$, which is given by the following form:

$$\begin{cases} x_1 = x_1(t_{k-1}) + (x_1(t_k) - x_1(t_{k-1}))\theta, \\ x_2 = x_2(t_{k-1}) + (x_2(t_k) - x_2(t_{k-1}))\theta, \\ x_3 = x_3(t_{k-1}) + (x_3(t_k) - x_3(t_{k-1}))\theta, \end{cases} \tag{4.7}$$

where (x_1, x_2, x_3) is the current point of L and θ is a parameter $(\theta \in \mathbb{R})$.

By substituting the expressions for x_1, x_2 and x_3 from Eq (4.7) into Eq (4.6), we obtain an equation in terms of θ, which is given by:

$$A^*\theta = B^*. \tag{4.8}$$

In (4.8)

$$\left.\begin{aligned} A^* =& h(b_{p+1} - b_p)(x_1(t_k) - x_1(t_{k-1})) - h(a_{p+1} - a_p)(x_2(t_k) - x_2(t_{k-1})) \\ &+ (a_p b_{p+1} - a_{p+1} b_p)(x_3(t_k) - x_3(t_{k-1})), \\ B^* =& h(a_p b_{p+1} - a_{p+1} b_p) - h(b_{p+1} - b_p)(x_1(t_{k-1}) \\ &+ h(a_{p+1} - a_p)x_2(t_{k-1}) - (a_p b_{p+1} - b_p a_{p+1})x_3(t_{k-1}), \end{aligned}\right\} \quad p = 1, \ldots, n.$$

In the given scenario, due to the existence of an intersection point, $A^* \neq 0$ and $y^j = (x_1(\theta), x_2(\theta), x_3(\theta))$, where $\theta = B^*/A^*$.

Finally, consider the following cases:

4) If $x_3(t_k) = 0$ and $(x_1(t_k), x_2(t_k)) \in S_{n+1}$ then $y^j = (x_1(t_k), x_2(t_k), 0)$.
5) If $x_3(t_k) < 0$, determine the intersection point $y(y_1, y_2, 0)$ of the plane $x_3 = 0$ with the line L that passes through the points $x(t_{k-1})$ and $x(t_k)$. Subsequently, if $(y_1, y_2, 0) \in \overline{S_{n+1}}$, then the intersection point is $y^j = (y_1, y_2, 0)$.

Remark 2. It is evident that the probability of the simulated Wiener process path passing exactly through a discontinuous line is practically zero. However, if during the computation, for any index j, the intersection point y^j happens to lie on the discontinuous line (a case accounted for in the computational algorithm), then $g(y^j) = 0$ will be used as the j-th term in the series in formula (3.2). Practically, we are ignoring this run.

5. An auxiliary classical problem

It is important to note that for the three-dimensional case, there are no exact test solutions available for generalized problems of type 1. Therefore, to verify the accuracy and reliability of the numerical solution scheme for Problem 1, we use the following approach.

If we set the boundary condition function (2.5) in 1 to be $g_i(y) = 1/|y - x^0|$, where $y \in S_i$ $(i = 1, \ldots, n+1)$, $x^0 = (x_1^0, x_2^0, x_3^0) \overline{\in} \overline{D}$, with $|y - x^0|$ denoting the distance between points y and x^0, then the curves l_k $(k = 1, \ldots, 2n)$ will act as removable discontinuity curves for the boundary function $g(y)$. In this case, rather than solving the generalized Problem 1, we effectively address a classical Dirichlet harmonic problem.

Problem 2. *Find a function $u(x) \equiv u(x_1, x_2, x_3) \in C^2(D) \cap C(\overline{D})$ satisfying the following conditions:*

$$\begin{aligned} \Delta u(x) &= 0, && x \in D, \\ u(y) &= 1/|y - x^0|, \qquad y \in S, && x^0 \overline{\in} \overline{D}. \end{aligned}$$

We address this problem using the MPS with an algorithm designed for Problem 1. It is established that Problem 2 is well posed, meaning that its solution exists, is unique, and continuously depends on the input data. The exact solution for Problem 2 is given by

$$u(x, x^0) = \frac{1}{|x - x^0|}, \qquad x \in \overline{D}, \quad x^0 \overline{\in} \overline{D}. \tag{5.1}$$

In addition to the above, the function $u(x, x^0)$ has the following properties:

(1) $u(x, x^0)$, as a function of x, with x^0 fixed, is a harmonic function in $\mathbb{R}^3$ everywhere except at the point x^0;
(2) $\lim_{x \to x^0} u(x, x^0) = \infty$;
(3) $\lim_{x \to \infty} u(x, x^0) = 0$;
(4) In the electrostatic interpretation, $u(x, x^0)$ represents the potential at point x in free $\mathbb{R}^3$ space due to a point charge of intensity $q = 4\pi C$ placed at point x^0;
(5) The function $u(x, x^0)$ is symmetric with respect to its arguments in free $\mathbb{R}^3$ space, i.e., $u(x, x^0) = u(x^0, x)$. This symmetry is a mathematical representation of the principle of reciprocity in physics: A source placed at x^0 exerts the same influence at point x as a source placed at x does at point x^0.

Note that the numerical solution of Dirichlet classical harmonic problems using the MPS is both intriguing and significant (see e.g., [4, 13, 17]. In the present paper, Problem 2 serves an auxiliary role, primarily to validate the reliability of the scheme and the associated program needed for solving Problem 1. We first solve Problem 2 and then compare the results with the exact solution of Problem 1, which is solved considering the boundary conditions (2.5).

In this present paper the MPS is applied to two examples. In the tables in the present paper (see Tables 1 to 4), N represents the number of trajectories in the simulated Wiener process for the given points $x^i = (x_1^i, x_2^i, x_3^i) \in D$, and nq denotes the quantification number. The tables below, display for the problem of type 2, the numerical absolute errors Δ^i of $u_N(x)$ as approximated by the MPS, at the points $x^i \in D$, for various values of nq and N. The results are presented in scientific notation.

In particular, $\Delta^i = max|u_N(x^i) - u(x^i, x^0)|$, $(i = 1, 2, \ldots, 5)$, where $u_N(x^i)$ represents the approximate solution of Problem 2 at the point x^i, as defined by formula (3.2), while the exact solution $u(x^i, x^0)$ of the test problem is given by Eq (5.1). The tables show the probabilistic solution $u_N(x)$ for Problem 1 at the points x^i, also defined by formula (3.2).

Remark 3. Problems of types 1 and 2 involving ellipsoidal, spherical, cylindrical, conic, prismatic, and regular pyramidal domains, as well as axially symmetric finite domains with cylindrical holes, external Dirichlet generalized problems for spheres, and special types of irregular pyramidal domains, are discussed in [18, 19, 21].

6. Numerical examples

Example 1. In this example the domain D is the interior of an irregular 3-sided pyramid $P_3(h)$, where h is the height and the coordinates of the vertices are $M = (0, 0, h)$, $A_1 = (a_1, b_1)$, $A_2 = (a_2, b_2)$, $A_3 = (a_3, b_3)$.

It is important to note that in these examples, all pyramids are positioned identically in the coordinate system $Ox_1x_2x_3$, as is described in Section 2.

For both types of Problems 1 and 2, we use $h = 2$, $A_1 = (3, 0)$, $A_2 = (0, 2)$, $A_3 = (-2, -2)$, and $x^0 = (0, 0, -4)$. In Problem 1 the boundary function $g(y) \equiv g(y_1, y_2, y_3)$ is given by

$$g(y) = \begin{cases} 3, & y \in S_1, \\ 2, & y \in S_2, \\ 1, & y \in S_3, \\ 4, & y \in S_4, \\ 0, & y \in l_k \quad (k = 1, \ldots, 6). \end{cases} \tag{6.1}$$

In Eq (6.1), S_i $(i = 1, 2, 3)$ and S_4 represent the lateral faces and the base of P_3, out of boundaries, respectively, while l_k $(k = 1, \ldots, 6)$ denote the edges of P_3. In this context, l_k are considered non-conductors (or dielectrics) in a physical sense.

In all the examples analyzed, we use the scheme described in Section 4 to determine the intersection points $y^j = (y_1^j, y_2^j, y_3^j)$ $(j = 1, \ldots, N)$ where the trajectory of the Wiener process intersects the surface S.

As previously mentioned, we first solve the auxiliary Problem 2 to validate the accuracy of calculation program for Problem 1.

Since the accuracy of the approximate solution $u_N(x)$ of the test Problem 2 using the MPS at any point $x \in D$ depends on the complexity of the problem domain, the location of point x in the domain D, and the values of numbers nq and N. Therefore, in considered examples, during the approximate solution of Problem 2, in the first place, for each point x, we find the optimal quantification number nq (by selection) in the sense of accuracy (see e.g., [20]).

Table 1 (see also Figure 1) displays the absolute errors Δ^i for the numerical solution $u_N(x)$ of the test Problem 2 at the points $x^i \in D$ $(i = 1, \ldots, 5)$.

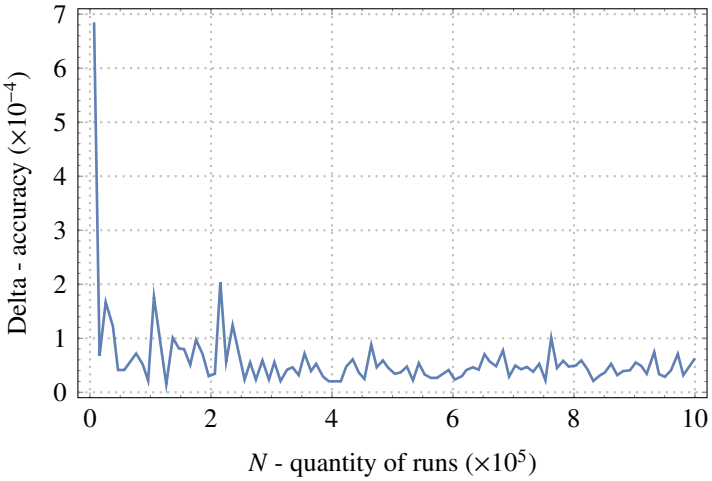

Figure 1. Results for Prolem 2 (Example 1) for starting point $(0, 0, 0.5)$.

Table 1. Results for Problem 2 (Example 1).

x^i	$(0, 0, 0.2)$	$(0, 0, 0.5)$	$(0, 0, 1)$	$(0, 0, 1.5)$	$(0, 0, 1.8)$
N	$\Delta^1, nq = 400$	$\Delta^2, nq = 200$	$\Delta^3, nq = 300$	$\Delta^4, nq = 400$	$\Delta^5, nq = 400$
$5E+3$	$0.21E-3$	$0.64E-3$	$0.18E-3$	$0.26E-3$	$0.43E-5$
$1E+4$	$0.17E-3$	$0.11E-3$	$0.11E-4$	$0.53E-4$	$0.51E-4$
$5E+4$	$0.35E-5$	$0.97E-4$	$0.94E-5$	$0.81E-4$	$0.32E-4$
$1E+5$	$0.53E-4$	$0.43E-5$	$0.81E-4$	$0.21E-4$	$0.26E-4$
$5E+5$	$0.44E-4$	$0.10E-5$	$0.39E-4$	$0.42E-4$	$0.19E-4$
$1E+6$	$0.37E-4$	$0.12E-5$	$0.28E-4$	$0.26E-4$	$0.25E-4$

Based on the numerical results shown in Table 1, we can confirm that the code for Problem 1 is correct. In Table 1, the interior points are chosen for the numerical experiment. Although any point can be selected, including those from the neighborhood of edges. This issue is discussed in more detail in [20].

Generally, increasing the values of nq and N enhances the accuracy of the solution. To achieve this, high-performance computing resources are required.

For this specific run, 13657 "very small" steps were required from the starting point to the intersection with the boundary of the pyramid (Figure 2). Solving the stated problem requires millions of such runs.

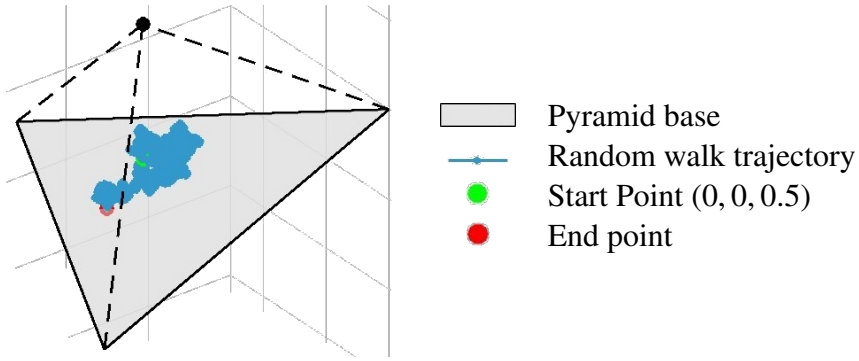

Figure 2. Illustration of single run for Problem 2 (Example 1) (13657 steps).

Table 2 presents the numerical solution $u_N(x)$ for Problem 1 at the same points x^i $(i = 1, \ldots, 5)$ along with the corresponding values of nq (refer to Table 1). The results demonstrate sufficient accuracy for many practical applications and align well with the expected physical behavior.

Table 2. Results for Problem 1 (Example 1).

x^i	$(0, 0, 0.2)$	$(0, 0, 0.5)$	$(0, 0, 1)$	$(0, 0, 1.5)$	$(0, 0, 1.8)$
N	$u_N(x^1)$	$u_N(x^2)$	$u_N(x^3)$	$u_N(x^4)$	$u_N(x^5)$
$5E+3$	3.42580	2.72620	1.99640	1.82100	1.77840
$1E+4$	3.43140	2.69770	2.00030	1.80340	1.79950
$5E+4$	3.42110	2.69890	2.01866	1.81518	1.79568
$1E+5$	3.42644	2.69704	2.01578	1.81060	1.79759
$5E+5$	3.42183	2.69627	2.01549	1.81343	1.79700
$1E+6$	3.42202	2.69564	2.01303	1.81354	1.79602

Example 2. In the present example, the domain D represents the interior of an irregular 8-sided pyramid $P_8(h)$ with $h = 2$. The coordinates of the vertices are $M(0, 0, 2)$, $A_1 = (2, 0)$, $A_2 = (1.5, 1)$, $A_3 = (0, 2)$, $A_4 = (-1, 2)$, $A_5 = (-2, 0)$, $A_6 = (-1.5, -1)$, $A_7 = (0, -2)$, $A_8 = (1, -1.5)$, and $x^0 = (0, 0, -4)$.

For Problem 1 the boundary function $g(y)$ is defined as follows:

$$g(y) = \begin{cases} 1, & y \in S_1, \\ 0, & y \in S_2, \\ 2, & y \in S_3, \\ 1, & y \in S_4, \\ 3, & y \in S_5, \\ 0, & y \in S_6, \\ 1, & y \in S_7, \\ 2, & y \in S_8, \\ 4, & y \in S_9, \\ 0, & y \in l_k \ (k = 1, \ldots, 16). \end{cases} \tag{6.2}$$

In Eq (6.2), S_i $(i = 1, \ldots, 8)$ and S_9 represent the lateral faces and the base of P_8 out of boundaries, respectively, while l_k $(k = 1, \ldots, 16)$ are the edges of P_8. Additionally, in this case the edges l_k and S_2, S_6 are non-conductors.

For Example 2, both Problems 2 and 1 were solved using the same parameters as in Example 1, specifically the points x^i $(i = 1, \ldots, 5)$ and numbers nq and N.

Table 3 displays the absolute errors Δ^i of the numerical solution $u_N(x)$ for the test Problem 2 at the points $x^i \in D$ $(i = 1, \ldots, 5)$.

Table 3. Results for Problem 2 (Example 2).

x^i	$(0, 0, 0.2)$	$(0, 0, 0.5)$	$(0, 0, 1)$	$(0, 0, 1.5)$	$(0, 0, 1.8)$
N	$\Delta_1, nq = 400$	$\Delta_2, nq = 200$	$\Delta_3, nq = 300$	$\Delta_4, nq = 400$	$\Delta_5, nq = 400$
$5E+3$	$0.26E-3$	$0.33E-3$	$0.15E-3$	$0.12E-4$	$0.12E-3$
$1E+4$	$0.24E-3$	$0.24E-3$	$0.31E-3$	$0.81E-4$	$0.22E-4$
$5E+4$	$0.77E-4$	$0.33E-4$	$0.10E-3$	$0.35E-4$	$0.52E-4$
$1E+5$	$0.50E-4$	$0.54E-4$	$0.74E-4$	$0.72E-4$	$0.96E-5$
$5E+5$	$0.49E-4$	$0.21E-4$	$0.40E-4$	$0.57E-4$	$0.29E-4$
$1E+6$	$0.48E-4$	$0.48E-4$	$0.31E-5$	$0.95E-5$	$0.16E-4$

Based on the numerical results presented in Table 3, we can confirm that the code for Problem 1 is correct.

Table 4 displays the approximate values of the solution $u_N(x)$ for Problem 1 at points x^i $(i = 1, \ldots, 5)$.

Table 4. Results for Problem 1 (in Example 2).

x^i	$(0, 0, 0.2)$	$(0, 0, 0.5)$	$(0, 0, 1)$	$(0, 0, 1.5)$	$(0, 0, 1.8)$
N	$u_N(x^1)$	$u_N(x^2)$	$u_N(x^3)$	$u_N(x^4)$	$u_N(x^5)$
$5E+3$	3.41100	2.57060	1.57640	1.13120	1.06340
$1E+4$	3.37220	2.54410	1.59120	1.13420	1.05030
$5E+4$	3.37734	2.56292	1.56556	1.13714	1.06130
$1E+5$	3.38355	2.55075	1.57076	1.13227	1.05812
$5E+5$	3.38580	2.55173	1.56809	1.13250	1.06473
$1E+6$	3.38650	2.55202	1.56873	1.13109	1.06451

The results are sufficiently accurate for many practical applications and align well with any physical process described by the Laplace equation.

In the present work we solved the problems of type 1 where the boundary functions $g_i(y)$ $(i = 1, \ldots, n+1)$ are constants. This choice was driven by the aim to evaluate how closely the calculation results match the physical reality. It is clear that solving Problem 1 under condition (2.5) is as easy as solving Problem 2. Generally, Problem 1 can be solved for configurations of discontinuity curves that allow us to identify the section of the surface S where the intersection point lies.

The analysis of numerical experiments demonstrates that the proposed algorithm is both reliable and effective for solving problems of types 1 and 2. In particular, the algorithm is notably straightforward to be implemented numerically.

7. Conclusions

(1) This study demonstrates that the proposed algorithm is exceptionally well-suited to solve approximately Problems 2 and 1. Notably, this algorithm can determine the solution at any point within the domain, a feature that distinguishes it from other algorithms discussed in the literature.
(2) A key advantage of the algorithm is that it does not require an approximation of the boundary function, which enhances its effectiveness.
(3) The algorithm is user-friendly to code, has low computational cost, and provides accuracy that meets the requirements of many practical problems.
(4) In future work, exploring the following areas is planned:
    - Applying the proposed algorithm to solve Dirichlet classical and generalized harmonic problems in an infinite $\mathbb{R}^3$ space with a finite number of spherical cavities.
    - Utilizing the MPS to tackle similar problems within finite domains enclosed by multiple closed surfaces.
    - Extending the MPS application to solve these problems in infinite 2D domains with a finite number of circular holes.
    - Implementing the MPS for solving these problems in regular and irregular prisms.

Author contributions

Conceptualization, M.Z., Z.T., N.K., and T.D.; methodology, M.Z., Z.T., N.K.,T.D., J.M.S., and F.C.-A.; formal analysis,M.Z., Z.T., N.K., T.D., and F.C.-A.; investigation,M.Z., Z.T., N.K.,T.D., J.M.S., and F.C.-A.; writing—original draft,M.Z., Z.T., N.K., and T.D.; writing—review and editing, J.M.S. and F.C.-A. All authors have read and agreed to the published version of the manuscript.

Use of Generative-AI tools declaration

The authors declare that they have not used Artificial Intelligence (AI) tools in the creation of this article.

Conflict of interest

The authors declare no conflicts of interest.

References

1. B. M. Budak, A. A. Samarski, A. N. Tíjonov, *Problemas de la física matemática. Tomo 1, 2*, Moscow: Mir, 1984. (Translated from the third Russian edition by José Ramil Alvarez).
2. H. S. Carslaw, J. C. Jaeger, *Conduction of heat in solids*, 2 Eds., New York: The Clarendon Press, Oxford University Press, 1959.
3. A. Chaduneli, Z. Tabagari, M. Zakradze, A computer simulation of probabilistic solution to the Dirichlet plane boundary problem for the Laplace equation in case of an infinite plane with a hole, *Bull. Georgian Acad. Sci.,* **171** (2005), 437–440.

4. A. Chaduneli, Z. Tabagari, M. Zakradze, On solving the internal three-dimensional Dirichlet problem for a harmonic function by the method of probabilistic solution, *Bull. Georgian Natl. Acad. Sci. (N.S.)*, **2** (2008), 25–28.
5. A. Chaduneli, M. V. Zakradze, Z. Tabagari, A method of probabilistic solution to the ordinary and generalized plane Dirichlet problem for the Laplace equation, *Proc. Sixth TSTC Scientific Advisory Committee Seminar*, **2** (2003), 361–366.
6. D. J. Griffiths, *Introduction to electrodynamics*, 4 Eds., Cambridge, UK: Cambridge University Press, 2017. https://doi.org/10.1017/9781108333511
7. L. V. Kantorovich, V. I. Krylov, *Approximate methods of higher analysis*, 3 Eds., New York: Interscience Publishers, Inc., 1964.
8. N. Koblishvili, Z. Tabagari, M. Zakradze, On reduction of the Dirighlet generalized boundary value problem to an ordinary problem for harmonic function, *Proc. A. Razmadze Math. Inst.*, **132** (2003), 93–106. Available from: `https://institutes.gtu.ge/uploads/20/v132-4.pdf`.
9. N. S. Koshlyakov, E. B. Glinerm, M. M. Smirnov, *Differential equations of mathematical physics*, Amsterdam: North-Holland Publishing Company, 1964.
10. M. Kublashvili, Z. Sanikidze, M. Zakradze, A method of conformal mapping for solving the generalized Dirichlet problem of Laplace's equation, *Proc. A. Razmadze Math. Inst.*, **160** (2012), 71–89. Available from: `https://institutes.gtu.ge/uploads/20/v160-6.pdf`.
11. W. B. Smythe, *Static and dynamic electricity*, New York, NY: Hemisphere Publishing, 1987.
12. M. Zakradze, N. Koblishvili, A. Karageorghis, Y. Smyrlis, On solving the Dirichlet generalized problem for harmonic function by the method of fundamental solutions, *Semin. I. Vekua Inst. Appl. Math. Rep.*, **34** (2008), 24–32. Available from: `https://institutes.gtu.ge/uploads/20/zakradze-v34.pdf`.
13. M. Zakradze, M. Kublashvili, N. Koblishvili, A. Chakhvadze, The method of probabilistic solution for determination of electric and thermal stationary fields in conic and prismatic domains, *Trans. A. Razmadze Math. Inst.*, **174** (2020), 235–246. Available from: `https://rmi.tsu.ge/transactions/TRMI-volumes/174-2/v174(2)-11.pdf`.
14. M. Zakradze, M. Kublashvili, Z. Sanikidze, N. Koblishvili, Investigation and numerical solution of some 3D internal Dirichlet generalized harmonic problems in finite domains, *Trans. A. Razmadze Math. Inst.*, **171** (2017), 103–110. http://dx.doi.org/10.1016/j.trmi.2016.11.001
15. M. Zakradze, M. Kublashvili, Z. Tabagari, N. Koblishvili, On numerical solving the Dirichlet generalized harmonic problem for regular n-sided pyramidal domains by the probabilistic method, *Trans. A. Razmadze Math. Inst.*, **176** (2022), 123–132. Available from: `https://rmi.tsu.ge/transactions/TRMI-volumes/176-1/v176(1)-10.pdf`.
16. M. Zakradze, B. Mamporia, M. Kublashvili, N. Koblishvili, The method of probabilistic solution for 3D Dirichlet ordinary and generalized harmonic problems in finite domains bounded with one surface, *Trans. A. Razmadze Math. Inst.*, **172** (2018), 453–465. http://dx.doi.org/10.1016/j.trmi.2018.08.005

17. M. Zakradze, Z. Sanikidze, Z. Tabagari, On solving the external three-dimensional Dirichlet problem for a harmonic function by the probabilistic method, *Bull. Georgian Natl. Acad. Sci.*, **4** (2010), 19–23. Available from: `http://science.org.ge/old/moambe/4-3/Zakradze.pdf`.

18. M. Zakradze, Z. Tabagari, N. Koblishvili, T. Davitashvili, J. M. Sanchez-Saez, F. Criado-Aldeanueva, The numerical solution of the external Dirichlet generalized harmonic problem for a sphere by the method of probabilistic solution, *Mathematics*, **11** (2023), 539. http://dx.doi.org/10.3390/math11030539

19. M. Zakradze, Z. Tabagari, M. Mirianashvili, N. Koblishvili, T. Davitashvili, The method of probabilistic solution for the Dirichlet generalized harmonic problem in irregular pyramidal domains, *Trans. A. Razmadze Math. Inst.*, **177** (2023), 475–483. Available from: `https://rmi.tsu.ge/transactions/TRMI-volumes/177-3/v177(3)-13.pdf`.

20. M. Zakradze, Z. Tabagari, M. Mirianashvili, N. Koblishvili, T. Davitashvili, On the solution of Dirichlet generalized and classical spatial harmonic problems by the MPS in neighborhood of the considered domain surface, *Bull. Tbilisi Int. Center Math. Inf.*, **28** (2024), 11–21. Available from: `https://www.emis.de/journals/TICMI/vol28_1/2.pdf`.

21. M. Zakradze, Z. Tabagari, Z. Sanikidze, E. Abramidze, Computer modelling of a probabilistic solution for the Dirichlet generalized harmonic problem in some finite axisymmetric bodies with a cylindrical hole, *Bull. TICMI*, **26** (2022), 37–52.

AIMS Press